⌘ *Author's Choice*

THE JOURNAL OF BIOLOGICAL CHEMISTRY VOL. 286, NO. 1, pp. 620–633, January 7, 2011

Negative Regulation of EGFR-Vav2 Signaling Axis by Cbl Ubiquitin Ligase Controls EGF Receptor-mediated Epithelial Cell Adherens Junction Dynamics and Cell Migration*

Received for publication, September 23, 2010 Published, JBC Papers in Press, October 12, 2010, DOI 10.1074/jbc.M110.188086

Lei Duan[‡§1], Srikumar M. Raja[‡§2], Gengsheng Chen[§3], Sumeet Virmani[§4], Stetson H. Williams[‡], Robert J. Clubb[‡5], Chandrani Mukhopadhyay[‡], Mark A. Rainey[‡§], Guoguang Ying[§6], Manjari Dimri[§7], Jing Chen[§8], Alagarsamy L. Reddi[§9], Mayumi Naramura[‡§], Vimla Band[‡§¶], and Hamid Band[‡§‖10]

From the [‡]Eppley Institute for Cancer and Allied Diseases, and Departments of [‖]Biochemistry and Molecular Biology, Pathology and Microbiology, Pharmacology and Neuroscience, and [¶]Genetics, Cell Biology and Anatomy, College of Medicine, University of Nebraska Medical Center, Omaha, Nebraska 68198-5950 and the [§]Department of Medicine, NorthShore University Health Systems, Northwestern University, Evanston, Illinois 60201

The E3 ubiquitin ligase Casitas B lymphoma protein (Cbl) controls the ubiquitin-dependent degradation of EGF receptor (EGFR), but its role in regulating downstream signaling elements with which it associates and its impact on biological outcomes of EGFR signaling are less clear. Here, we demonstrate that stimulation of EGFR on human mammary epithelial cells disrupts adherens junctions (AJs) through Vav2 and Rac1/Cdc42 activation. In EGF-stimulated cells, Cbl regulates the levels of phosphorylated Vav2 thereby attenuating Rac1/Cdc42 activity. Knockdown of Cbl and Cbl-b enhanced the EGF-induced disruption of AJs and cell motility. Overexpression of constitutively active Vav2 activated Rac1/Cdc42 and reorganized junctional actin cytoskeleton; these effects were suppressed by WT Cbl and enhanced by a ubiquitin ligase-deficient Cbl mutant. Cbl forms a complex with phospho-EGFR and phospho-Vav2 and facilitates phospho-Vav2 ubiquitinylation. Cbl can also interact with Vav2 directly in a Cbl Tyr-700-dependent manner. A ubiquitin ligase-deficient Cbl mutant enhanced the morphological transformation of mammary epithelial cells induced by constitutively active Vav2; this effect requires an intact Cbl Tyr-700. These results indicate that Cbl ubiquitin ligase plays a critical role in the maintenance of AJs and suppression of cell migration through down-regulation of EGFR-Vav2 signaling.

EGFR[11] is a prototype receptor tyrosine kinase (RTK) that controls fundamental cellular functions such as cell proliferation, differentiation, survival, adhesion, and migration. EGFR regulates these diverse cell functions through interactions with and activation of a number of downstream signaling proteins that organize multilayered, distinctive, and interconnected signaling pathways (1–6). The magnitude and duration of these signaling pathways as well as their spatial distribution need to be delicately controlled to maintain cellular homeostasis during growth factor stimulation. Indeed, uncontrolled signaling due to RTK overexpression or mutational activation or aberrant activation of downstream effectors are linked to the pathogenesis of cancer (3, 6–9).

Ligand-initiated EGFR signaling is spatio-temporally restricted by internalization and lysosomal degradation of activated receptors (10–12). The Casitas B lymphoma protein (Cbl) family E3 ubiquitin ligases (Cbl, Cbl-b, and Cbl-c) negatively regulate activated RTKs, including EGFR, by facilitating the ubiquitinylation-dependent sorting of activated receptors to lysosomes (10, 12–15). Cbl proteins are recruited to activated EGFR primarily by direct binding of the N-terminal TKB domain to phosphorylated tyrosine residue 1045 in EGFR (15) and by indirect recruitment through the adaptor protein Grb2 (16). The Cbl-bound activated EGFR is ubiquitinylated and recognition of ubiquitin signal by the endosomal

* This work was supported, in whole or in part, by National Institutes of Health Grants CA87986, CA99163, CA105489, and CA116552 (to H. B.) and CA94143 and CA96844 (to V. B.). This work was also supported by Department of Defense Breast Cancer Research Grants W81XWH-05-1-0231, DAMD17-02-1-0508, and W81XWH-07-1-0351 (to V. B.), Nebraska Department of Health and Human Services Grant LB-506 (to S. M. R.), and Nebraska Center for Nanomedicine-Center for Biomedical Research Excellence Grant NCN-COBRE (seed grant to S. M. R.).

⌘ *Author's Choice*—Final version full access.

[1] To whom correspondence may be addressed: Dept. of Radiation Oncology, Rush University Medical Center, 1750 W Harrison St, Chicago, IL 606612. E-mail: lei_duan@rush.edu.

[2] To whom correspondence may be addressed: Eppley Institute for Research in Cancer and Allied Diseases, University of Nebraska Medical Center, 985950 Nebraska Medical Center, Omaha, NE 68198-5950. E-mail: sraja@unmc.edu.

[3] Present address: Coskata Energy, Warrenville, IL 60555.

[4] Present address: Dept. of Radiology, Northwestern University Feinberg School of Medicine, Chicago, IL 60611.

[5] Present address: Genzyme Genetics, Westborough, MA 01581.

[6] Present address: Tianjin Hospital and Cancer Institute, Tianjin Medical University, West HuanHu Road, HeXi District, Tianjin, China.

[7] Present address: Dept. of Biochemistry, George Washington University School of Medicine, Washington, D.C. 20037.

[8] Present address: Dept. of Pathology, Northwestern University Feinberg School of Medicine, Chicago, IL 60611.

[9] Present address: Dept. of Medicine, Northwestern University Feinberg School of Medicine, Chicago, IL 60611.

[10] To whom correspondence may be addressed: Eppley Institute for Research in Cancer and Allied Diseases, University of Nebraska Medical Center, 985950 Nebraska Medical Center, Omaha, NE 68198-5950. E-mail: hband@unmc.edu.

[11] The abbreviations used are: EGFR, EGF receptor; RTK, receptor tyrosine kinase; MEC, mammary epithelial cell; AJ, adherens junction; GEF, guanine nucleotide exchange factor; MTT, 3-(4,5-dimethylthiazol-2-yl)-2,5-diphenyltetrazolium bromide; KD, knockdown; DOX, doxycycline; SH2, Src homology domain 2; IP, immunoprecipitation.

protein complex required for transport (ESCRT) protein complexes facilitates sorting of the receptor into inner vesicles of the multivesicular body for eventual lysosomal degradation (17–19). In this fashion, Cbl proteins attenuate RTK signaling by direct down-regulation of the activated receptor.

In addition to their direct interaction with RTKs and regulation of RTK traffic, Cbl proteins also form complexes with signaling intermediates that play key roles in cellular activation. Evidence in lymphocyte activation systems, driven by non-RTK-coupled antigen receptors, suggests that Cbl proteins can orchestrate the ubiquitinylation-dependent negative regulation of nonreceptor signaling components such as PI3K (through interaction with p85 subunit), the Rap G-protein guanine nucleotide exchange factor (GEF) C3G (via Cbl protein interaction with Crk adaptor proteins), and Rho GTPase GEF Vav (11, 20–22). However, the importance of the interactions of Cbl proteins with these nonreceptor signaling proteins has not been examined downstream of RTKs. Recent findings have revealed that, in addition to lysosomal sorting of RTKs, interaction with Cbl can also result in negative regulation of the phospholipase C-γ1 pathway downstream of PDGF receptor and VEGF receptor apparently through competition between Cbl and phospholipase C-γ1 for a shared binding site on the receptor (23, 24). However, whether Cbl proteins negatively regulate RTK signaling by ubiquitin-dependent regulation of downstream signaling proteins remains unclear.

Although negative regulation of EGFR by Cbl has been well established in model cell systems, the biological impact of such negative regulation and the EGFR effectors that are impacted in physiologically relevant cellular systems remains unexplored. Human MECs are uniquely EGF-dependent for proliferation (25). Similar to other epithelial cell systems, apical-basolateral polarity in MECs is generated and maintained through specific cell-cell junctions and cell-substratum adhesions that are important for epithelial function and homeostasis (26–28). The basolateral E-cadherin-containing AJs are critical in the organization of epithelial polarity and tissue morphogenesis and play important roles in epithelial cell differentiation, proliferation, and migration (29–31). Disruption of AJs is also linked to cancer development and metastasis (32–34). Notably, ligand-activated EGFR can phosphorylate cadherin complexes, leading to the disassembly of AJs (35). EGFR can also down-regulate E-cadherin through stimulation of E-cadherin endocytosis (36).

One key pathway downstream of RTKs that remodels AJs involves the activation of Rho GTPases. These small GTPases cycle between GTP-bound active forms and GDP-bound inactive forms under the influence of GEFs and GTPase-activating proteins, respectively (37–39). Activation of RhoA and Rac1 is involved in cell scattering upon stimulation through c-MET, a well studied model of epithelial cell dissociation (40, 41). Activation of Rac1 alone is sufficient to disrupt AJs (42). Stimulation through EGFR is also known to activate Rho GTPases (43, 44). A key signaling pathway through which EGFR activates Rho GTPases involves Vav family Rho GEFs, Vav1–3 (43–46). Vav proteins interact directly with the phosphorylated EGFR through their C-terminal SH2 domains and are subsequently activated by EGFR-dependent phosphorylation of tyrosine residues located in their N-terminal acidic regions (47, 48). Among the Vav family proteins, Vav2 is ubiquitously expressed and has been characterized in model cell systems as a GEF for Rho, Rac1, and Cdc42 downstream of EGFR (44, 46). We have shown that Vav2 plays a critical role in the disruption of MEC polarity downstream of EGFR (49).

Previously, we have shown that Cbl can negatively regulate the hematopoietically restricted Vav1 protein through ubiquitinylation, resulting in attenuation of T-cell receptor signaling (22). Cbl directly interacts with Vav1 based on the Vav1 SH2 domain binding to phosphorylated tyrosine residue 700 in the C-terminal region of Cbl (50). Given the structural similarity of Vav1 and Vav2 and the involvement of Vav2 downstream of EGFR as a regulator of Rho GTPases, we explored the potential Cbl interaction with and regulation of Vav2 function as a paradigm to understanding the biological impact of Cbl-mediated negative regulation of EGFR signaling pathways in a physiologically relevant setting.

EXPERIMENTAL PROCEDURES

Antibodies and Other Reagents—Rabbit anti-Vav2 peptide antisera were generated against Vav2 peptide sequence 208–222 (QETEAKYYRTLEDIE) through a commercial vendor (Animal Pharma Inc., Yakima, WA). Monoclonal antibodies against EGFR (clone 528; ATCC) and E-cadherin (clone E4.6; gift of Drs. Michael Brenner and Jonathan Higgins, Brigham and Women's Hospital, Boston) were purified from mouse hybridoma supernatants using Protein-G columns. Purified anti-phosphotyrosine (anti-Tyr(P)) antibody 4G10 was a gift from Dr. Brian Druker (Oregon Health Sciences University, Portland). The following antibodies were commercially obtained: monoclonal anti-RhoA from Santa Cruz Biotechnology; anti-Rac1 from Cytoskeleton; anti-β-actin from Sigma; polyclonal anti-Cdc42 from Cell Signaling; and anti-Cbl, anti-Cbl-b, and anti-phospho-Vav2 from Santa Cruz Biotechnology. Alexa Fluor 594-conjugated phalloidin was from Invitrogen.

Small Hairpin RNA (shRNA) Constructs and cDNAs—The shRNA target sequences in genes of interest were identified using the on-line S-fold software, blasted against the NCBI database to minimize off-target possibilities, and cloned (together with scrambled sequences as controls) into pSuper-.retro retroviral vector (OligoEngine Inc.). The sequences of shRNAs are as follows: AAGAGCATCTCCACCTCTA (control), GAAAGCCTGCCACGATAAA (Vav2 #1), GAAGATGACAAGAGGAACT (Vav2 #2), GGTTGTGTCAGAACCCAAA (Cbl #2), GGCGAAACCTAACCAAACT (Cbl #4), and GACCATACCTCATAACAAG (Cbl-b). A murine cDNA encoding Vav2 was cloned into lentiviral vector pLenti6/V5-Dest (Invitrogen). The C-terminally YFP-tagged Vav2 (obtained from the Signaling Consortium) was subcloned into retroviral vector pRevTRE (Invitrogen) through an engineered SalI site. The wild type and mutant Cbl expression plasmids in pMSCV-pac retroviral vector (BD Biosciences) have been described previously (13). Cbl shRNA#2.

MEC Cell Lines and Culture—The HPV16-E6/E7-immortalized 16A5 (51) and spontaneously immortalized MCF10A

(52) human MEC lines were maintained in DFCI-1 medium, which contains 12.5 ng/ml EGF, as described previously (51). The MCF10A cell lines stably expressing pSuper.retro-driven shRNAs or lentivirus-driven murine Vav2 were generated using standard viral packaging and infection strategies. The transduced cells were selected and maintained in DFCI-1 medium supplemented with puromycin (0.5 μg/ml), G418 (500 μg/ml), or hygromycin (100 μg/ml) antibiotics and used as polyclonal cell lines. The 16A5-Tet-On-YFP-Vav2-Y172F cell line has been described previously (49).

Immunoprecipitations (IPs)—IPs from the indicated amounts of cell lysate protein were performed using protein A-Sepharose 4B beads (Amersham Biosciences) as an immunosorbent. For immunodepletion studies, cell lysates were serially incubated (for 2–3 rounds) with aliquots of specific or control Abs together with protein A-Sepharose 4B beads, and the resulting immunodepleted or mock-depleted (control) supernatants were used for further IPs. For analyses of ubiquitinylation, cell lysates were prepared in the RIPA buffer (50 mM Tris, pH 7.2, 1% Triton X-100, 0.5% sodium deoxycholate, 0.1% SDS, 150 mM sodium chloride) with 1 mM sodium orthovanadate, 10 mM NaF, and 0.1 mM PMSF. For co-IPs, the lysis buffer contained 1% Triton X-100 as a detergent, 50 mM Tris, pH 8.0, 2 mM EDTA, and protease/phosphatase inhibitors, as in the RIPA lysis buffer.

GST Pulldown of Activated RhoA, Rac1, and Cdc42—GTP-bound forms of RhoA, Rac1, or Cdc42 were pulled down using bacterially expressed, purified GST-RBD (Rho-binding domain of rhotekin; interacts with GTP-bound RhoA) or GST-PBD (p21-binding domain of PAK; interacts with GTP-bound Rac1 and Cdc42) respectively, as described previously (49). Cells were washed with ice-cold PBS and lysed in the RIPA buffer. The cell lysates were rocked at 4 °C for 10 min and clarified of insoluble material by centrifugation at 16,000 × *g* at 4 °C for 10 min. Equal aliquots of lysate proteins were incubated with glutathione-Sepharose beads coated with 20–30 μg of purified GST-RBD or GST-PBD fusion proteins at 4 °C for 45 min. The beads were washed four times with the wash buffer (50 mM Tris, pH 7.5, 1% Triton X-100, 150 mM NaCl, 10 mM $MgCl_2$, and 1 mM PMSF). Bound RhoA, Rac, or Cdc42 proteins were detected using Western blotting.

Confocal Immunofluorescence Microscopy—For immunofluorescence analysis, cells were cultured on glass coverslips, fixed in 4% formaldehyde/PBS, permeabilized with 0.5% Triton X-100 for 5 min, and stained with anti-E-cadherin antibody followed by Alexa Fluor 488-conjugated secondary Abs together with Alexa Fluor 594-conjugated phalloidin to stain actin. The stained cells were mounted in Vectashield mounting medium (Vector Laboratories), and images were acquired with a confocal microscope (Nikon C1 or Zeiss confocal LSM 510) under ×400 or ×600 magnifications.

Quantification of Junctional Actin Cytoskeleton Reorganization—3×10^3 cells were grown on 20 × 20-mm glass coverslips in DFCI-1 medium without EGF for 4 days to allow the formation of discrete cell colonies. The cells were stimulated with 3 ng/ml EGF for 12 h before fixation, permeabilized with 0.5% Triton X-100, and stained with Alexa Fluor 594-conjugated phalloidin. The cells were then scanned using confocal microscopy at the subapical plane to acquire cell junctional F-actin images. To quantify junctional F-actin distribution and reorganization, the segmented histogram (Metamorph software) was used to subgroup the F-actin staining according to fluorescence intensity. Using a typical EGF-starved colony and a typical EGF-stimulated cell colony in the control cell line as standards to configure the Bin fluorescence intensity range (see the example in Fig. 4*C*), the F-actin populations were subgrouped as circumferential, perijunctional, and diffuse. The Bin area of each group was measured, and the percentage Bin area of the circumferential F-actin *versus* the total F-actin was calculated and graphed.

Subcellular Fractionation—Membrane and cytosolic fractions, used for the assessment of phosphorylated Vav2 recruitment to membranes, were prepared with commercial kits (Thermo Fisher Product 78840 or Q-proteome catalog no. 37502), using manufacturers' protocols. The kits were supplemented with sodium orthovanadate (1 mM) as a phosphatase inhibitor.

Assay of Cell Proliferation Using MTT Dye Incorporation—Cells were plated in 96-well plates (2000 cells/well) at day 0 and cultured in DFCI-1 medium without or with EGF (12.5 ng/ml) from day 1. MTT dye incorporation was assessed from day 2 to day 5 using a commercial kit (Invitrogen). The MTT absorbance values were acquired with a microplate reader at 570 nm wavelength.

Statistical Analysis—One-way analysis of variance and Student's *t* test were used to determine the statistical significance of differences among experimental groups. Student's *t* test was used to determine the statistical significance between control and experimental groups.

RESULTS

EGF Stimulation Reorganizes Junctional Actin Cytoskeleton and Disrupts AJs in MECs—When immortal nontumorigenic human MEC lines 16A5 and MCF10A are grown as monolayer cultures in DFCI-1 medium without EGF, they form relatively tight colonies; two-color confocal immunofluorescence microscopy analysis of polymerized actin and E-cadherin at the subapical plane revealed typical circumferential actin cables and continuous E-cadherin staining at cell-cell junctions (Fig. 1, *A* and *B*, *upper panels*), indicating that these cells form AJs. However, upon EGF stimulation, the cells became flattened and less tightly attached to each other; the circumferential actin cables were disrupted and reorganized into more widely distributed shorter actin bundles flanking the cell-cell junctions, and E-cadherin staining showed an interrupted pattern (Fig. 1, *A* and *B*, *lower panels*); the latter results indicate that signaling via the EGFR induces junctional actin cytoskeleton reorganization and disruption of AJs. We therefore used this system to evaluate the impact of perturbing Cbl protein expression.

Knockdown of Cbl Plus Cbl-b Enhances the EGF-induced Actin Cytoskeleton Reorganization, Disruption of AJs and Cell Migration, but Not Cell Proliferation—Knockdown (KD) of Cbl expression in MCF10A MEC line using either of two distinct shRNAs (shRNAs 2 and 4) led to a nearly complete loss of Cbl expression (Fig. 2*A*); EGFR degradation in response to

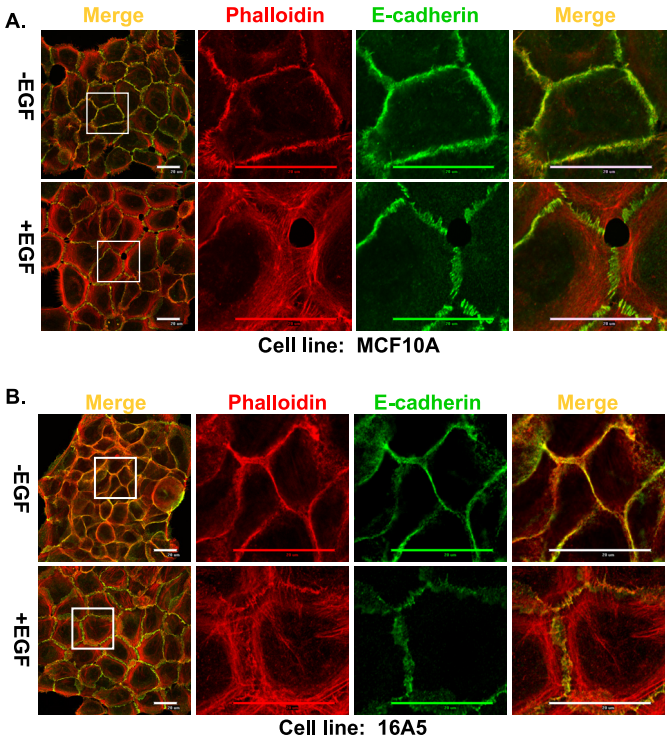

FIGURE 1. **EGF stimulation of MECs results in remodeling of junctional actin cytoskeleton and disruption of AJs.** MCF10A cells (*A*) and 16A5 cells (*B*) were grown without EGF for 4 days and stimulated with EGF (3 ng/ml) for 12 h. The cells were immunostained and scanned with confocal microscopy at the subapical plane for E-cadherin (*green*) or actin (phalloidin; *red*). Both the whole cell colony image and the high resolution image of the indicated areas in the colonies are presented (*scale bar,* 20 μm).

EGF stimulation was slightly delayed in both Cbl KD cell lines compared with a control shRNA-expressing cell line (Fig. 2*A*). Because Western blots for Cbl-b revealed that this protein is also expressed in MECs, and Cbl-b is also known to regulate EGFR degradation (14), we further generated MCF10A cells with stable KD of both Cbl and Cbl-b. Analysis of these cells shows a nearly complete lack of Cbl expression and an over 80% Cbl-b knockdown (Fig. 2*B*). EGF-induced EGFR ubiquitinylation was markedly reduced (Fig. 2*C*), and EGFR degradation was substantially delayed in Cbl and Cbl-b double-KD MCF10A cells (Fig. 2*D*).

Notably, EGF stimulation of MCF10A-Cbl/Cbl-b KD cells induced a markedly more robust reorganization of junctional actin cytoskeleton and cell scattering with a nearly complete loss of AJ staining (anti-E-cadherin) in a majority of cells compared with control KD cells (Fig. 2*E*). Furthermore, compared with control KD cells, the MCF10A-Cbl/Cbl-b KD cells exhibited markedly accelerated EGF-dependent cell migration in wound healing as well as Boyden chamber assays (Fig. 2, *F* and *G*). Similar results were observed in 16A5 MECs with stable knockdown of Cbl plus Cbl-b (data not shown). Notably, however, Cbl plus Cbl-b KD did not significantly affect the EGF-dependent cell proliferation (Fig. 2*H*) suggesting that Cbl proteins may more selectively attenuate EGFR-mediated disruption of cell-cell adhesion and cell migration. Notably, E-cadherin protein level was not changed by EGF stimulation or by Cbl plus Cbl-b knockdown in MCF10A cells (data not shown), indicating that EGF-induced disruption of AJs in MECs is not through down-regulation of E-cadherin.

EGF-induced Phosphorylation of Vav2 and Translocation to Cell-Cell Adhesion Sites—Studies in model cell systems have shown that Vav2 functions as a Rho family GEF and an actin cytoskeleton organizer downstream of EGFR (44, 46). We found that Vav2 is the predominant or only detectable Vav family protein in a number of MECs and breast cancer cell lines (data not shown). EGF stimulation of both MEC lines MCF10A and 16A5 resulted in rapid Vav2 tyrosine phosphorylation that waned over time (Fig. 3*A*). In addition, phosphorylated EGFR co-immunoprecipitated with Vav2 (Fig. 3*A*), and conversely, Vav2 was detected in anti-EGFR IPs (Fig. 3*B*).

As stimulation of MECs with EGF induced the remodeling of junctional actin, we hypothesized a role for Vav2 in the activation of Rho GTPases and remodeling of actin structures at cell-cell junctions. To test whether Vav2 is recruited to cell-cell junctions, we stably expressed a YFP-tagged Vav2 protein in MCF10A cells and examined its co-localization with EGFR, E-cadherin, or F-actin, using confocal imaging. Without EGF stimulation, YFP-Vav2 nearly exclusively localized to the cytoplasm (Fig. 3*C*). Following EGF stimulation, YFP-Vav2 localized to cell-cell junctions where it co-localized with EGFR (Fig. 3*C*), E-cadherin (Fig. 3*D*), and junctional F-actin (Fig. 3*D*). EGFR was expectedly internalized into endosomal vesicles within a few minutes of EGF stimulation (Fig. 3*C*); some Vav2-YFP co-localized with internalized EGFR, whereas a significant fraction remained at cell-cell junctions after the EGFR internalization (Fig. 3*C*). Membrane fractionation experiments following EGF stimulation further revealed that phospho-Vav2 was recruited to the cell membrane in response to EGF stimulation (Fig. 3, *E* and *G*); EGFR and phospho-EGFR served as markers for the membrane fraction (Fig. 3, *E* and *G*). A pool of phospho-Vav2 was also found in the cytosolic fraction (Fig. 3, *F* and *H*); this fraction was devoid of any associated EGFR. These results confirm our immunofluorescence-based analyses indicating the membrane recruitment of Vav2 and further show that the phosphorylated form of Vav2 that is induced upon EGF stimulation is recruited to the membrane.

Vav2 Is Critical for EGF-induced Rac1 and Cdc42 Activation, Reorganization of Junctional Actin Cytoskeleton, and Cell Migration in MECs—To assess if Vav2 plays a role in EGF-induced Rho GTPase activation in MECs, we established cell lines with stable knockdown of Vav2 (Fig. 4*A*, *lanes 3–6*). Stimulation with EGF induced the activation of RhoA, Rac1, as well as Cdc42 in control shRNA-expressing MECs (Fig. 4*A*, *lanes 1* and *2*). However, contrary to earlier results in model cells (44, 46) but consistent with recent results in a pancreatic epithelial cancer cell line (53), knockdown of Vav2 with two different shRNAs dramatically reduced the Rac1 and Cdc42 but not the RhoA activation in response to EGF (Fig. 4, *A* and *B*).

Because activated Rac1 is able to disrupt AJs in keratinocytes (42), we hypothesized a role of Vav2 in the disruption of AJs downstream of EGFR. To test the role of endogenous Vav2 in EGF-induced reorganization of junctional actin cytoskeleton, EGF-starved 16A5 cells stably expressing a control shRNA or two distinct Vav2 shRNAs (Fig. 4*D*) were stimu-

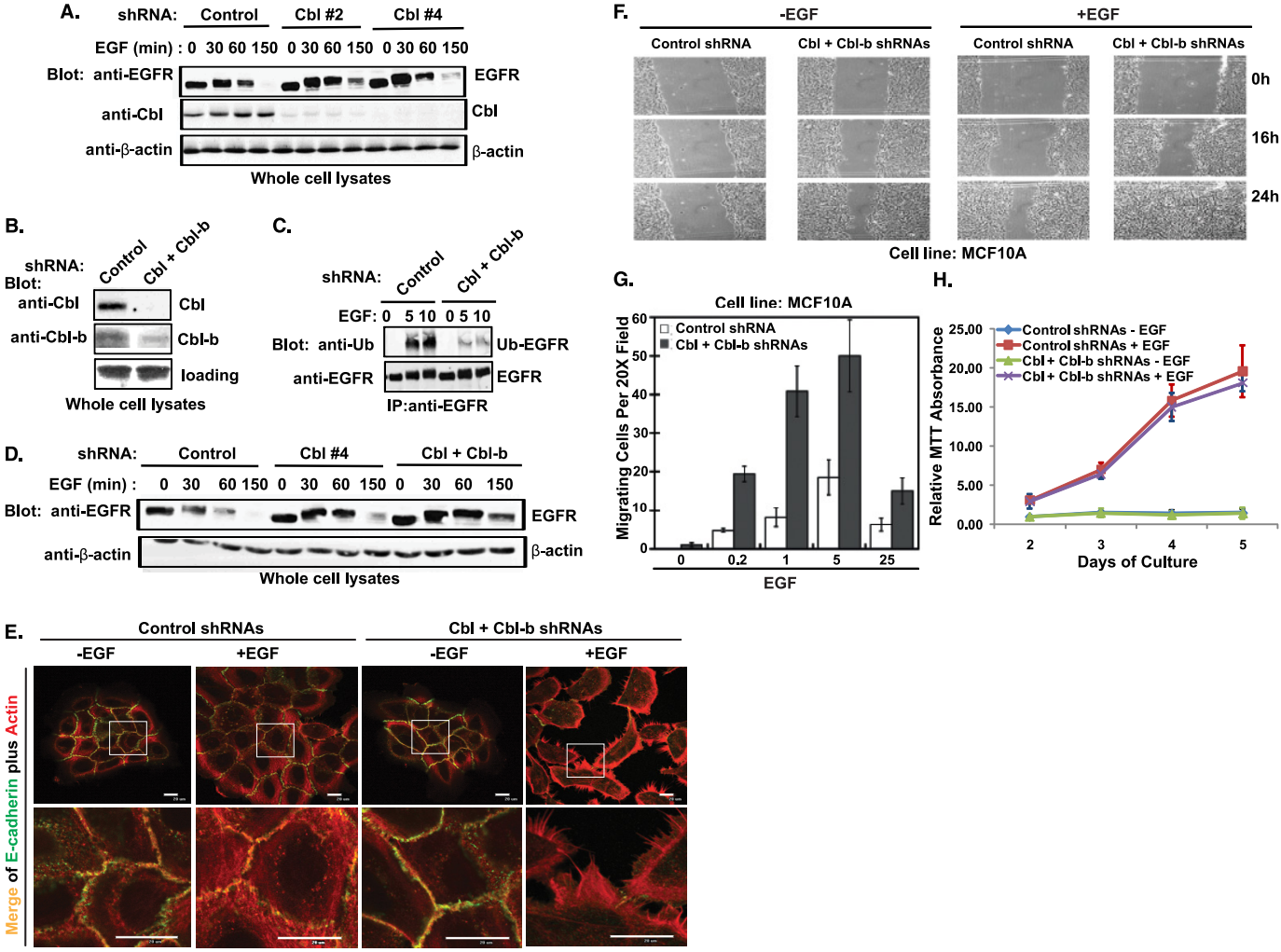

FIGURE 2. **Knockdown of Cbl and Cbl-b in MECs decreases the EGF-induced EGFR ubiquitinylation and degradation, enhances the disruption of AJs and cell migration, but does not affect cell proliferation.** *A,* MCF10A cells with stable expression of control shRNA, Cbl shRNA#2, and Cbl shRNA#4 were growth factor-starved for 3 days before stimulation with EGF (100 ng/ml) for the indicated time points. Whole cell lysates were immunoblotted for EGFR, Cbl, and β-actin. *B,* whole cell lysates of MCF10A cells with stable overexpression of control shRNAs or Cbl/Cbl-b shRNAs were immunoblotted for Cbl and Cbl-b. *C,* MCF10A cells with stable expression of control shRNAs or Cbl/Cbl-b shRNAs were growth factor-starved and stimulated with EGF (100 ng/ml) for the indicated time points. Cell lysates were subjected to IP with anti-an EGFR antibody and immunoblotted for ubiquitin (*upper panel, Ub-EGFR*) and EGFR (*lower panel*). *D,* MCF10A cells with control shRNA, Cbl shRNA (*#4*), or Cbl/Cbl-b shRNA expression were growth factor-starved for 3 days and stimulated with EGF (100 ng/ml) for the indicated time points. Whole cell lysates were immunoblotted for EGFR. *E,* MCF10A cells with control shRNA or Cbl/Cbl-b shRNA expression were growth factor-starved and then stimulated with EGF (3 ng/ml) for 12 h. The cells were immunostained with anti-E-cadherin antibodies (*green*) and phalloidin (*red*). Both the whole cell colony image and the high resolution image of the indicated areas in the colonies were acquired by confocal microscopy scanning at the subapical plane (*scale bar,* 20 μm). *F,* wound healing assay. MCF10A cells were grown to confluence and growth factor-starved for 72 h; a scratch wound was made with a micropipette tip (blue tip) and the edge of cells was marked. EGF (10 ng/ml) was then added to the starvation media, and cells were allowed to migrate toward the center of the wound and photographed at the indicated times (representative figure of three independent experiments). *G,* trans-well migration assay. Cells were growth factor-starved for 72 h, harvested, plated in the top chamber of trans-well plates (1×10^4 per chamber in triplicate) on a fibronectin-coated surface with 8-μm pores, and allowed to attach for 4 h. EGF at the indicated concentrations (ng/ml) was added to starvation media in the bottom well, and cells that migrated to the bottom side of the filter in 16 h were scored. Mean values are presented with standard deviation indicated. *H,* MCF10A cells with control shRNA or Cbl/Cbl-b shRNA expression were grown in 96-well plates (2×10^3/well) in octuplicates in DFCI media with or with EGF. MTT assay was done at the indicated days, and the average MTT absorbance values in each cell line were normalized to the non-EGF-treated cells harvested at day 2 and presented as a *graph* with standard deviation indicated (representative figure of three independent experiments). There is no statistically significant difference ($p = 0.34$) between the two groups.

lated with EGF and analyzed for junctional actin and E-cadherin staining. Indeed, circumferential actin cables were largely maintained and less peri-junctional short actin bundles were induced in response to EGF in Vav2 KD cells as compared with control shRNA cells (Fig. 4*D*), indicating that Vav2 is required for EGF-induced remodeling of junctional actin cytoskeleton. As the Vav2 KD phenotype was less profound than Rac1 or Cdc42 KD phenotype, we quantified the defect in actin reorganization in Vav2 KD cells using segmentation and subgroup analysis of junctional F-actin (details in Fig. 4*C,* legend). Indeed, the EGF-induced reorganization of junctional actin (reduction in circumferential F-actin as a percentage of total F-actin) was statistically significant in control shRNA-expressing cells (Fig. 4*E*, $p = 0.043$; paired *t* test) but not in either of the two Vav2 shRNA KD cell lines (Fig. 4*E*, $p = 0.45$ or 0.77). Similarly, the disruption of E-cadherin-mediated cell-cell junctions was less pronounced in Vav2 KD cells (Fig. 4*E*, compare the two Vav2 KD cell lines with con-

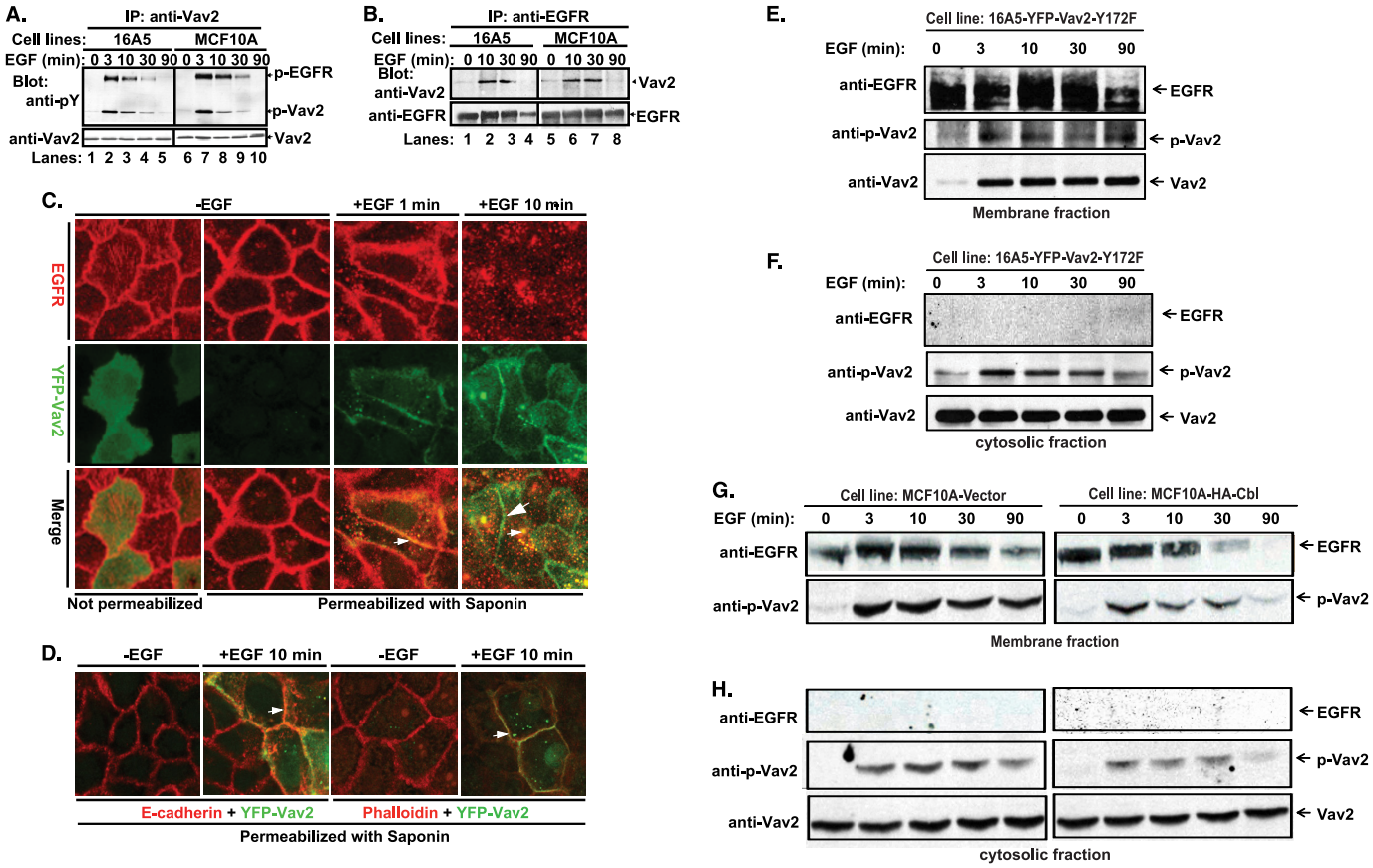

FIGURE 3. **EGF-induced phosphorylation of Vav2, association with EGFR, translocation of phospho-Vav2 to the cell membrane, and co-localization of Vav2 with EGFR, E-cadherin, or F-actin at cell-cell junctions.** *A,* growth factor-starved 16A5 (*lanes 1–5*) or MCF10A (*lanes 6–10*) cells were stimulated with EGF (100 ng/ml). The whole cell lysates were immunoprecipitated (*IP*) with anti-Vav2 Abs and immunoblotted with anti-phosphotyrosine (*pY*) Abs and anti-Vav2 Abs or (*B*) IP with anti-EGFR Abs (clone 528) and immunoblot for Vav2 and EGFR. *C,* MCF10A cells with stable expression of YFP-Vav2 WT (*green*) were growth factor-starved and stimulated with EGF (100 ng/ml). The cells were either fixed directly (*1st image* from *left*) or permeabilized with saponin/PBS (10 μg/ml, *2nd* to *4th images*) for 10 min before fixation and then immunostained for EGFR (*red*). The *yellow* color indicates co-localization of YFP-Vav2 with EGFR (*small arrowheads*); the *green* color indicates cell junction-localized Vav2 (*large arrowhead*). *D,* cells were permeabilized as above and immunostained for E-cadherin (*red, 1st* and *2nd images* from *left*) or F-actin (*red, 3rd* and *4th images*). The *yellow* color indicates the co-localization of YFP-Vav2 with E-cadherin or F-actin (*small arrowheads*). *E–H,* growth factor-starved 16A5-YFP-Vav2–172F cells (*E* and *F*) or vector-expressing *versus* WT Cbl-overexpressing MCF10A cells (*G* and *H*) were stimulated with EGF (100 ng/ml) for the indicated time points. Whole cell lysates were subjected to subcellular fractionation. Membrane (*E* and *G*) and cytosolic (*F* and *H*) fractions were immunoblotted for EGFR, phospho-Vav2, and Vav2.

trol cells). Notably, KD of Vav2 did not change E-cadherin protein levels as assessed by Western blotting (data not shown). Consistent with its role in modulating actin cytoskeleton remodeling, KD of Vav2 in either MCF10A or 16A5 MECs significantly decreased the EGF-dependent cell migration when analyzed using the wound-healing assay (data not shown).

Cbl, EGFR, and Vav2 Form a Complex—We have previously reported that Cbl interacts with EGFR in MECs (54). We have also shown that Cbl forms a complex with Vav1 through phosphorylated Cbl tyrosine 700, which binds to Vav1 SH2 domain; this interaction leads to Cbl-dependent Vav1 ubiquitinylation (22). We therefore hypothesized that Cbl may interact with the EGFR-Vav2 complex in EGF-stimulated cells. Indeed, endogenous Cbl was found to co-IP with Vav2 in response to EGF stimulation of growth factor-starved MCF10A cells (Fig. 5*A*). To further examine the nature of Vav2-Cbl association, we established MCF10A cell lines stably expressing HA-tagged WT Cbl or Cbl-Y700F mutant, as well as a vector control cell line; notably, the Cbl-Y700F mutant expression level is about 5-fold higher than that of WT HA-Cbl (Fig. 5, *B* and *D*). Anti-HA IP followed by anti-Vav2 immunoblotting revealed that Vav2 co-immunoprecipitated with both WT HA-Cbl and HA-Cbl-Y700F mutant following EGF stimulation (Fig. 5*B*). Because HA-Cbl-Y700F also co-immunoprecipitated with Vav2, we surmised that the co-IP was a reflection of a ternary complex of Cbl, EGFR, and Vav2. In this model, both Vav2 and Cbl could associate with phospho-EGFR via their SH2 or TKB domains, respectively. Alternatively, there is also a possibility of a linear ternary complex of EGFR-Cbl-Vav2. To assess if this was the case, we performed co-IP analysis using cell lysates from which EGFR was immunodepleted. Indeed, either anti-Vav2 blotting of anti-HA IPs or anti-HA blotting of anti-Vav2 IPs revealed a distinct decrease in Cbl and Vav2 co-IP in EGFR-depleted lysates suggesting that a majority of Vav2 and Cbl association is through a ternary complex with EGFR. However, a small residual pool of Vav2 was found to be associated with WT-HA-Cbl but not with HA-Cbl-Y700F following EGFR depletion (Fig. 5, *C* and *D*). These results indicate that Cbl interacts with two pools of Vav2 as follows: a major one is through a ternary complex formed by binding of Cbl and Vav2 to EGFR

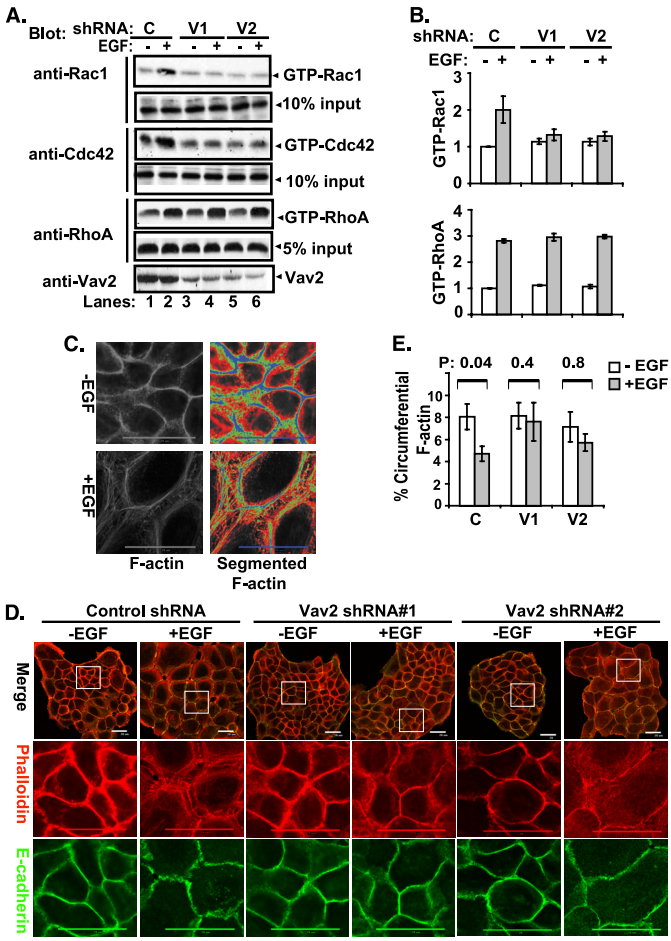

FIGURE 4. **EGF-induced reorganization of junctional actin cytoskeleton through activation of Vav2-Rac1/Cdc42.** *A,* control shRNA- (*C, lanes 1* and *2*), Vav2 shRNA#1- (*V1, lanes 3* and *4*), and Vav2 shRNA#2 (*V2, lanes 5* and *6*)-expressing cells were growth factor-starved for 72 h and stimulated with EGF (100 ng/ml) for 10 min. The whole cell lysates were subjected to GST-PBD or GST-RBD pulldown and immunoblotted for Rac1, Cdc42, or RhoA as indicated. The whole cell lysate input for pulldown was used as loading control and also blotted for Vav2 (*lowest panel*) (representative figure of three independent experiments). *B,* average relative density of GTP-bound forms of the Rac1 and RhoA from three experiments is presented as *bars* with standard deviation. *C,* quantification of junctional actin cytoskeleton reorganization. 3×10^3 cells were grown on 20 × 20-mm glass coverslips in DFCI-1 media without EGF for 4 days until the cells formed discrete colonies; the cells were then stimulated with EGF (3 ng/ml) for 12 h before fixation. The cells were permeabilized with 0.5% Triton X-100, stained with Alexa Fluor 594-conjugated phalloidin, and scanned under a confocal microscope at the subapical plane to acquire the junctional F-actin images. To quantify the distribution and reorganization of junctional F-actin, the segmented histogram (Metamorph software) was used to subgroup the F-actin staining according to the fluorescence intensity. Two typical cell images were used as the gold standard to configure the segmentation criteria in terms of fluorescence intensity (*FI*), which subgroups the junctional F-actin into circumferential (*blue*, *FI* = 255–161), peri-junctional (*green*, *FI* = 160–101), diffuse (*red*, *FI* = 100–61), and background (*black*, *FI* = 61–0). The Bin areas of each group were acquired, and the total Bin areas excluding background were used as total F-actin area, and the percentage Bin area of the circumferential F-actin *versus* the total F-actin was calculated and graphed. *D,* 16A5 cells with stable expression of control shRNA or Vav2 shRNAs were growth factor-starved for 4 days and stimulated with EGF (3 ng/ml) for 12 h. The cells were immunostained for E-cadherin (*green*) and F-actin (*red*) and were scanned with confocal microscopy at the subapical plane to acquire images of the whole cell colonies or of the indicated areas. *E,* cells with or without EGF stimulation (3 ng/ml for 12 h) were analyzed by F-actin segmentation. The mean percentage of circumferential F-actin in each experimental group was calculated from randomly selected colonies ($n = 19$) and the mean percentages were compared by one-way analysis of variance and then by paired *t* test following a logarithmic transformation. The mean percentages of the circumferential F-actin are presented with standard errors as *Y*-error bars, and the *p* values are indicated *above* the paired bars.

and a minor pool is dependent on phosphorylated tyrosine 700 in Cbl. The pool of Vav2 associated with EGFR and Cbl as a complex was phosphorylated (Fig. 5*E, lane 2*). However, the pool of Vav2 associated with Cbl as a separate complex (Fig. 5*E, lane 4*) showed no detectable phosphorylation, despite the fact that Cbl-Vav2 interaction occurred upon EGF stimulation (Fig. 5*E*). This suggests a possible direct interaction between the Vav2 SH2 domain and phospho-Cbl. Phospho-Vav2 IP after EGFR immunodepletion (Fig. 5*E, right panel*) confirmed the presence of a pool of phospho-Vav2 that was not associated with EGFR as also seen in analyses of the membrane fractions (Fig. 3, *G* and *H*).

Cbl Attenuates the EGFR-mediated Phosphorylation of Vav2 and Activation of Rac1/Cdc42—Given our results that Cbl and Vav2 form a complex, together with our previous studies that Cbl-Vav1 interaction promotes Vav1 ubiquitinylation (22), we reasoned that association with Cbl may promote Vav2 ubiquitinylation, resulting in attenuation of EGF-induced and Vav2-dependent activation of Rac1/Cdc42.

Overexpression of WT HA-Cbl in MCF10A cells reduced and shortened the EGF-induced phosphorylation of Vav2 (Fig. 5*F*). In contrast, overexpression of ubiquitin ligase-deficient HA-Cbl-C3AHN mutant prolonged the phosphorylation of Vav2 (Fig. 5*F*). Consistent with these results, EGF-induced phospho-Vav2 signals were reduced in the membrane (Fig. 3*G*) as well as cytosolic fractions (Fig. 3*H*) of Cbl-overexpressing cells. Consistent with these results, overexpression of WT HA-Cbl diminished whereas that of HA-Cbl-C3AHN enhanced the EGF-induced Rac1 activation (Fig. 6, *A* and *B*). In contrast, combined Cbl and Cbl-b KD dramatically enhanced the EGF-induced Vav2 phosphorylation in response to EGF stimulation (Fig. 5*G*) and enhanced the EGF-induced Rac1 and Cdc42 activation (Fig. 6, *A* and *B*). Consistent with the role of Cbl in attenuating Vav2-Rac1/Cdc42 activation, overexpression of WT Cbl attenuated the EGF-induced reorganization of junctional actin cytoskeleton and disruption of AJs (Fig. 6*C*).

Cbl Attenuates the Activation of Rac1/Cdc42 and Reorganization of Junctional Actin Cytoskeleton Induced by the Overexpression of Constitutively Active Vav2—To directly test whether Cbl can attenuate the function of Vav2, we stably introduced the constitutively active Vav2-Y172F mutant together with wild type Cbl or Cbl mutants into MCF10A cells (Fig. 7, *A* and *B*). Stable overexpression of the Vav2-Y172F mutant caused the enlargement and flattening of cells with disruption of cell-cell adhesions (Fig. 7*C*). However, the cell-cell junctions in these cells were maintained when WT Cbl was co-overexpressed (Fig. 7*C*). In contrast, transduction of the ubiquitin ligase-deficient mutants Cbl-C3AHN or Cbl-70Z into Vav2-Y172F-overexpressing cells accentuated the Vav2-Y172F-dependent phenotype resulting in enhanced morphological transformation of cells; the cells became extremely enlarged and spread out, with almost complete loss of epithelial morphology and cell-cell junctions (Fig. 7*C*). Surprisingly, however, these cells proliferated poorly, and we have not been able to propagate them for further analysis. Interestingly, introduction of Cbl mutants (C3AHN/Y700F or 70Z/Y700F) disabled for direct interaction with Vav2 through

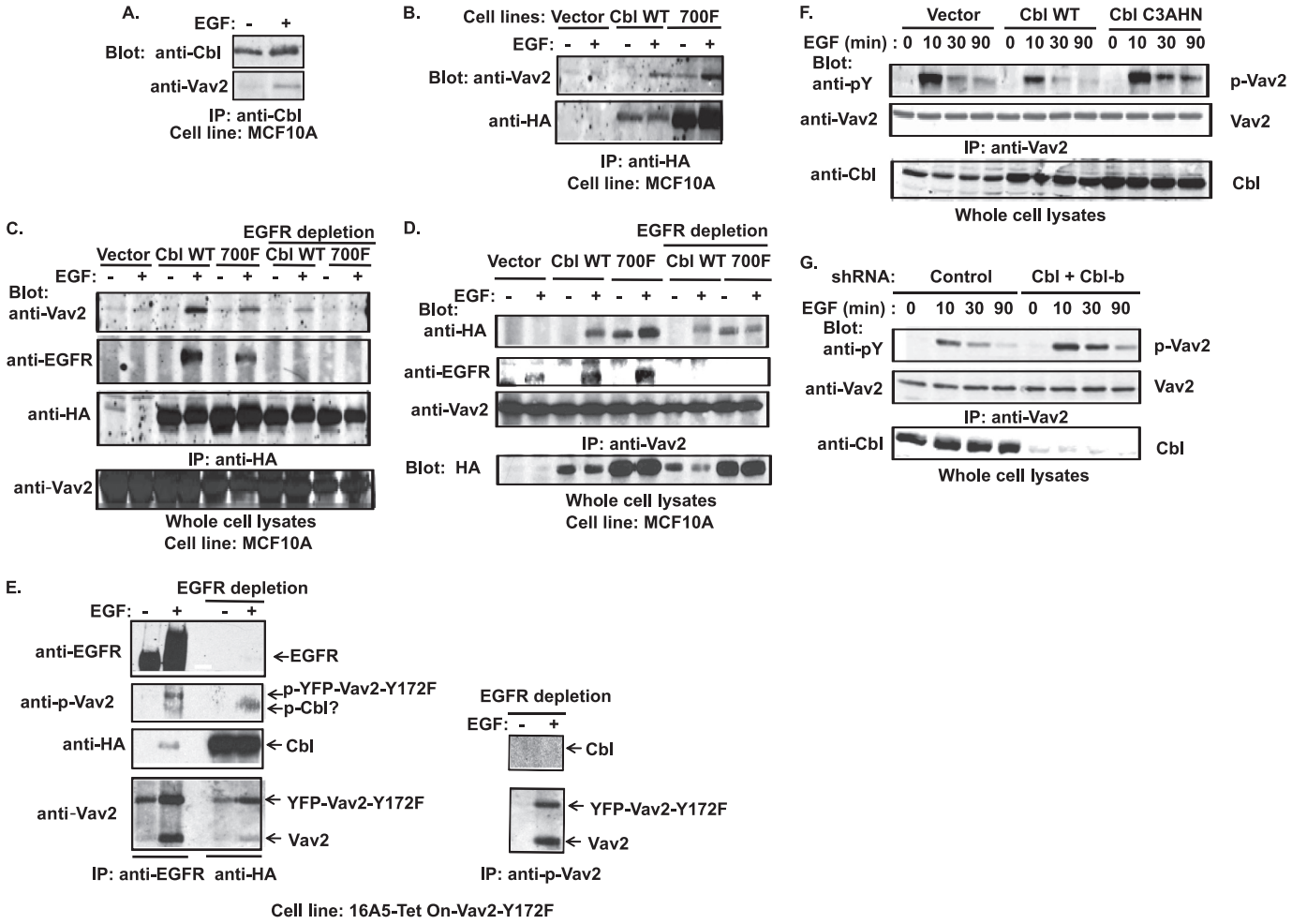

FIGURE 5. **EGF-induced Cbl-Vav2 association and Cbl-dependent attenuation of Vav2 phosphorylation.** *A,* growth factor-starved MCF10A cells were stimulated with EGF (100 ng/ml) for 10 min, and anti-Cbl IPs from whole cell lysates were immunoblotted for Vav2 and Cbl. *B,* MCF10A cells with stable overexpression of HA-tagged wild type Cbl or Cbl-Y700F were stimulated with EGF (100 ng/ml) for 10 min and anti-HA IPs immunoblotted for Vav2. *C,* equal amount of cell lysates from the cells with vector or wild type Cbl overexpression and one-third amount of cell lysates from cells with Cbl-Y700F expression prepared under the same experimental conditions as described in *B* were subjected to IP (*1st* to *6th lanes*) with anti-HA Abs as such or after immunodepletion of EGFR before (*7th* to *10th lanes*) and then immunoblotted for Vav2, EGFR, and HA. *D,* equal amounts of cell lysates from vector-, wild type Cbl-, or Cbl-Y700F-overexpressing cells under the same experimental conditions as described in *B* were subjected to IP with anti-Vav2 Abs (*1st* to *6th lanes*) or immunodepleted of EGFR before IP with anti-HA Abs (*7th* to *10th lanes*) followed by immunoblotting for HA, EGFR, and Vav2. *E,* growth factor-starved and DOX-induced 16A5-Tet-On-Vav2-Y172F/HA-Cbl-expressing cells were treated with EGF (100 ng/ml) for 5 min. Equal amounts of cell lysates were subjected to serial (three times) anti-EGFR IP to immunodeplete EGFR (*left panel, 1st* and *2nd lanes*) before IP with anti-HA (*left panel, 3rd* and *4th lanes*) or with anti-phospho-Vav2 antibodies (*right panel*) and immunoblotted for EGFR, phospho-Vav2, Vav2, and HA. *F,* growth factor-starved MCF10A cells with stable overexpression of vector, wild type Cbl or Cbl-C3AHN mutant were stimulated with EGF (100 ng/ml) for the indicated time. Equal amounts of cell lysates were subjected to IP with anti-Vav2 Abs and immunoblotted for Tyr(P) (*pY*) and Vav2. Whole cell lysates were also blotted for Cbl (*lowest panel*). *G,* MCF10A cells with stable expression of control shRNAs or Cbl/Cbl-b shRNAs were stimulated with EGF (100 ng/ml). Cell lysates were subjected to IP with anti-Vav2 Abs and blotted for Tyr(P) (*pY*) and Vav2. Whole cell lysates were also immunoblotted for Cbl (*lowest panel*).

Tyr-700 of Cbl into Vav2-Y172F-overexpressing cells induced only moderate morphological transformation (Fig. 7*C*). This result implies that the interaction of Cbl-C3AHN or Cbl-70Z mutants with Vav2-Y172F mutant through tyrosine 700 serves to enhance Vav2 function.

Because stable cell lines co-overexpressing E3-deficient mutants of Cbl and Vav2-Y172F mutant could not be established, we used a tetracycline-inducible (Tet-On) expression system that we have recently established in 16A5 MECs (16A5-Tet-On-172F) (49). In this system, the expression of YFP-tagged constitutively active Vav2-Y172F mutant is under tetracycline control. WT Cbl or its mutants were stably introduced into 16A5-Tet-On-172F cells (Fig. 7*D*). Doxycycline (DOX)-induced overexpression of the Vav2-Y172F mutant in 16A5-Tet-On-172F cells led to an increase in activated Rac1 (Fig. 7*F*). The induced Rac1 activation was suppressed by the co-overexpressed WT Cbl and to a lesser extent by the Cbl-Y700F mutant (note that WT Cbl and Cbl-Y700F mutant expression levels are similar in 16A5-Tet-On-172F cells) but not by the Cbl-C3AHN mutant (Fig. 7*F*). KD of Cbl using two different shRNAs (Fig. 7*E*) enhanced the Vav2-Y172F-induced activation of Rac1 (Fig. 7*G*).

Consistent with the Rac1 activation results, vector control cells with induced overexpression of Vav2-Y172F mutant showed thinner and shorter peri-junctional actin fibers with less discernable circumferential actin rings (Fig. 7*H*). Cells with overexpression of WT Cbl largely maintained the circumferential actin rings with less peri-junctional actin bundle

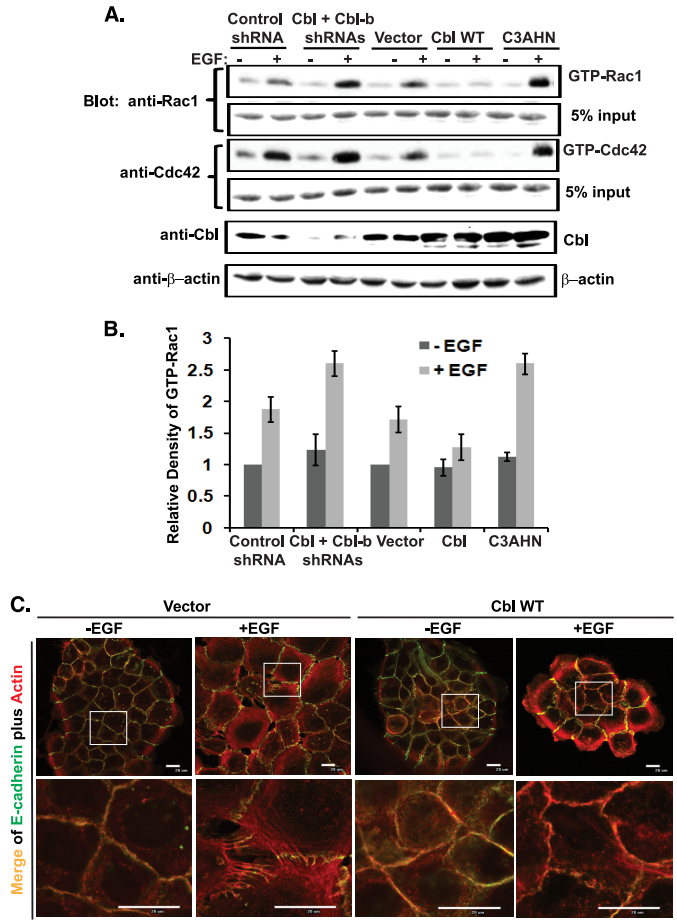

FIGURE 6. **Role of Cbl in attenuating Rac1 and Cdc42 activation and remodeling of cell-cell junctions in response to EGF stimulation of MECs.** *A,* MCF10A cells with stable expression of control shRNAs, Cbl/Cbl-b shRNAs (*right panel*), vector, wild type Cbl, or Cbl-C3AHN were stimulated with EGF (100 ng/ml) for 10 min. Cell lysates were subjected to GST-PBD pulldown and immunoblotted for Rac1 and Cdc42 (representative figure of three independent experiments). *B,* average density of the GTP-bound Rac1 from three independent experiments is presented as a *bar graph* with S.D. as *error bars*. *C,* growth factor-starved MCF10A cells with stable overexpression of vector or wild type Cbl were stimulated with EGF (100 ng/ml) for 12 h. The cells were immunostained with anti-E-cadherin Abs (*green*) and phalloidin (*red*). Both whole cell colony image and the high resolution image of the indicated areas in the colonies were acquired by confocal microscopy scanning at the subapical plane.

formation; this effect is less pronounced in Cbl-Y700F mutant-overexpressing cells (Fig. 7*H*). In contrast, overexpression of the Cbl-C3AHN mutant led to a dramatic enlargement of Vav2-Y172F-overexpressing cells, and this effect was accompanied by the formation of abundant thinner and shorter peri-junctional actin fibers (Fig. 7*H*). These results further confirm the conclusions that E3-deficient Cbl mutants enhance Vav2 activity and that this is dependent on Tyr-700-mediated interaction with Vav2.

WT Cbl but Not the Y700F or Ubiquitin Ligase-deficient Mutants of Cbl Enhance the Ubiquitinylation of YFP-Vav2-Y172F—The above results suggest that Cbl negatively regulates Vav2 signaling by a mechanism that requires the Cbl E3 activity. Our efforts to detect the ubiquitinylation of endogenous Vav2 upon EGF stimulation of MCF10A cells were not successful (data not shown), most likely due to weak signals as less than 0.1% of the total pool of Vav2 associated with Cbl (Fig. 5*C,* compare the co-immunoprecipitated Vav2 in the *4th* or *6th lanes* with 1% lysate input in the *lower panel*). We therefore used the 16A5-Tet-On-172F cell lines with stable overexpression of vector, WT Cbl, Cbl-Y700F mutant, or Cbl-C3AHN mutant to assess the ubiquitinylation of overexpressed Vav2-Y172F in these cells. The cells were treated with DOX for 3 days to induce the expression of Vav2-Y172F and then treated with DMSO (control) or the proteasome inhibitor MG132 for 4 h. Anti-ubiquitin blotting of anti-Vav2 IPs revealed an increase in ubiquitin signals in MG132-treated 16A5-Tet-On-172F cells, which was enhanced by WT Cbl overexpression (Fig. 8, *A* and *B*), but to a lesser extent by Cbl-Y700F overexpression (Fig. 8*A*), and was reduced by Cbl-C3AHN mutant overexpression (Fig. 8*A*) or knockdown of Cbl (Fig. 8*B*). MG132 treatment caused the accumulation of Cbl proteins (Fig. 8, *A* and *B, Cbl* blot), which is consistent with known auto-ubiquitinylation and auto-degradation of Cbl proteins (55, 56). To further test whether phospho-Vav2 is ubiquitinylated by Cbl, 16A5-Tet-On-YFP-Vav2-Y172F cells were stimulated with EGF in the presence or absence of MG132. Phospho-Vav2 IPs were performed from lysates subjected to EGFR immunodepletion (two rounds of anti-EGFR IP). Anti-ubiquitin blotting of anti-phospho-Vav2 IPs revealed EGF stimulation-dependent ubiquitinylation, which was significantly increased by Cbl overexpression (Fig. 9*A*). The cell lysates remaining after anti-phospho-Vav2 IP (phospho-Vav2 depleted) were further subjected to total Vav2 IP and immunoblotted for ubiquitin (Fig. 9*B*, *2nd* to *5th* and *7th* to *10th lanes*). Compared with anti-Vav2 IPs of nondepleted cell lysate (Fig. 9*B*, *1st* and *6th lanes*), the anti-Vav2 IP of phospho-Vav2-depleted cell lysate showed a significantly lower ubiquitin signal. These results suggest that Cbl-dependent ubiquitinylation predominantly occurs on the phosphorylated pool of Vav2.

DISCUSSION

Biochemical and cell biological evidence has clearly established the Cbl family ubiquitin ligases as crucial determinants of activated RTK ubiquitinylation and subsequent lysosomal degradation, thereby implicating Cbl family proteins as negative regulators of RTK signaling (11–15, 57). EGFR has been a widely studied model RTK in this context, but such studies have been limited to model cell systems and analyses of early biochemical signaling events (13–16). Relatively little is known at present about the cell biological consequences of Cbl E3-dependent negative regulation of EGFR in physiologically relevant cell systems. A second major area of lack of knowledge relates to the role of Cbl family protein-mediated negative regulation of EGFR traffic *versus* the effects of Cbl proteins at the level of intermediate signaling machinery whose components form complexes with Cbl proteins. Studies reported here address these two key issues in a physiologically relevant model of EGFR-mediated biological regulation using nontumorigenic human MECs.

Human MECs in culture are dependent on EGFR activation for continued proliferation, and stimulation of EGFR also regulates other critical cellular behaviors in these cells (25). We focused on the EGFR activation-dependent modulation of

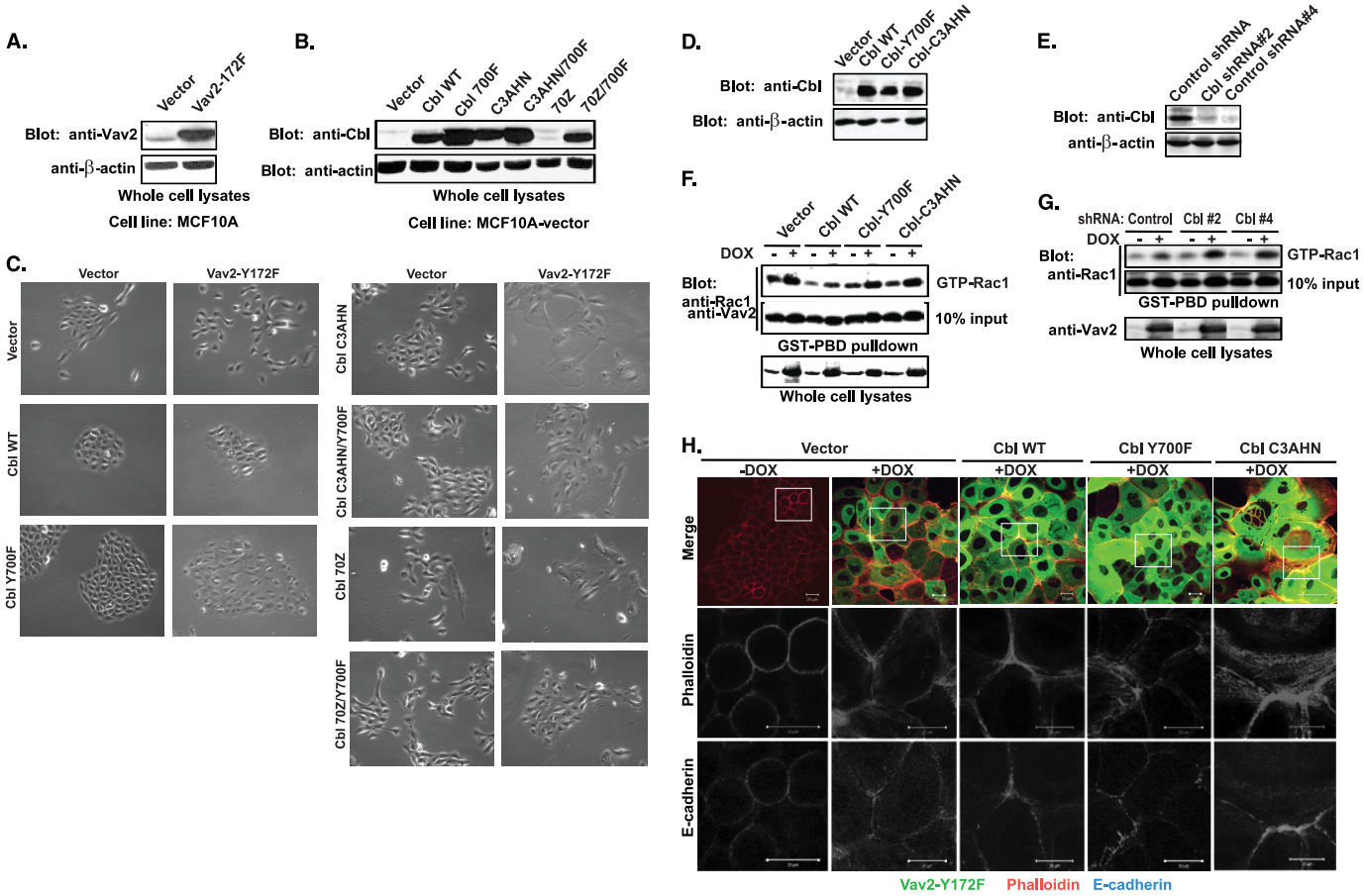

FIGURE 7. **Suppression of the constitutively active Vav2-Y172F mutant-mediated morphological transformation, activation of Rac1, and reorganization of junctional actin cytoskeleton by WT Cbl but not by E3-deficient mutants.** *A,* whole cell lysates of MCF10A cells with stable expression of vector or Vav2-Y172F mutant were Western-blotted for Vav2. *B,* lysates of MCF10A cells with stable transduction of vector, wild type Cbl, or Cbl mutants were Western-blotted for Cbl. *C,* vector- or Vav2-Y172F-expressing MCF10A cells were stably transduced with vector, wild type Cbl, or Cbl mutants and selected with antibiotics for 2 weeks. The selected cells were trypsinized and replated at low density and cultured for 1 week. Cells were photographed with a phase-contrast light microscope under transmitted light. *D–H,* whole cell lysates of 16A5-Tet-On-172F cells with stable expression of vector, wild type Cbl, Cbl-Y700F, and Cbl-C3AHN (*D*) or stable expression of control shRNA, Cbl shRNA#2, and Cbl shRNA#4 (*E*) were immunoblotted for Cbl and β-actin. The cells were treated with vehicle or DOX for 3 days to induce Vav2 expression, and whole cell lysates were subjected to GST-PBD pulldown assay and immunoblotted for Rac1 (*F* and *G*). *H,* 16A5-Tet-On-172F cells with stable expression of vector, wild type Cbl, Cbl-Y700F, and Cbl-C3AHN were grown in DFCI media without EGF and treated with vehicle or DOX for 3 days. The cells were immunostained with anti-E-cadherin Abs (*blue*) and phalloidin (*red*). Both whole cell colony image and the high resolution image of the indicated areas in the colonies were acquired by confocal microscopy scanning at the subapical plane.

cell-cell junctions and migration (35, 36) as these are biological traits relevant to normal homeostasis as well as tumorigenesis and metastasis (32, 34, 58–62). Importantly, the known modulation of these biological behaviors by Rho family of GTPases (39, 42, 63–69) allowed us to specifically examine the role of Cbl E3 ligases in the context of a potential downstream signaling pathway mediated by Vav2. As we show here, stimulation of MECs through EGFR controls cell-cell junctions, junctional actin cytoskeleton remodeling, and cell migration largely through activation of the Vav2 signaling axis. This conclusion is supported by overexpression as well as complementary shRNA strategies.

Our results using combined KD of Cbl and Cbl-b or ectopic expression of specific mutants of HA-tagged Cbl provide strong support for a role of Cbl E3 ligases as negative regulators of the main Vav family member expressed in MECs, Vav2. The consequences of this negative regulation are that Cbl proteins function in attenuating EGFR signaling that normally culminates in Rac/Cdc42 activation through Vav2 to disrupt cell-cell junctions, remodel actin cytoskeleton, and promote cell migration. The attenuation of EGFR-mediated activation of Rac1 and Cdc42 correlates primarily with the duration of Vav2 phosphorylation. As we show that ubiquitinylation of Vav2 and its phosphorylated pool is dependent Cbl E3-ligase activity, it is reasonable to conclude that Cbl proteins attenuate Vav2-dependent Rho GTPase activation by accelerating the ubiquitinylation and degradation of Vav2. However, in view of the findings that a major pool of the Cbl-Vav2 complex is part of a ternary complex with EGFR, it is likely that attenuation of Vav2 function is in part a reflection of the overall negative regulation of activated EGFR by Cbl proteins. This suggestion is consistent with our findings that Vav2, and in particular its phosphorylated (active) pool, is recruited to the membrane and associates with EGFR upon EGF stimulation and our observation that a fraction of Vav2 appears to remain associated with EGFR as it undergoes endocytic trafficking.

Curiously, our immunofluorescence and subcellular fractionation studies also reveal a proportion of Vav2, which includes phospho-Vav2, that appears not to be associated with

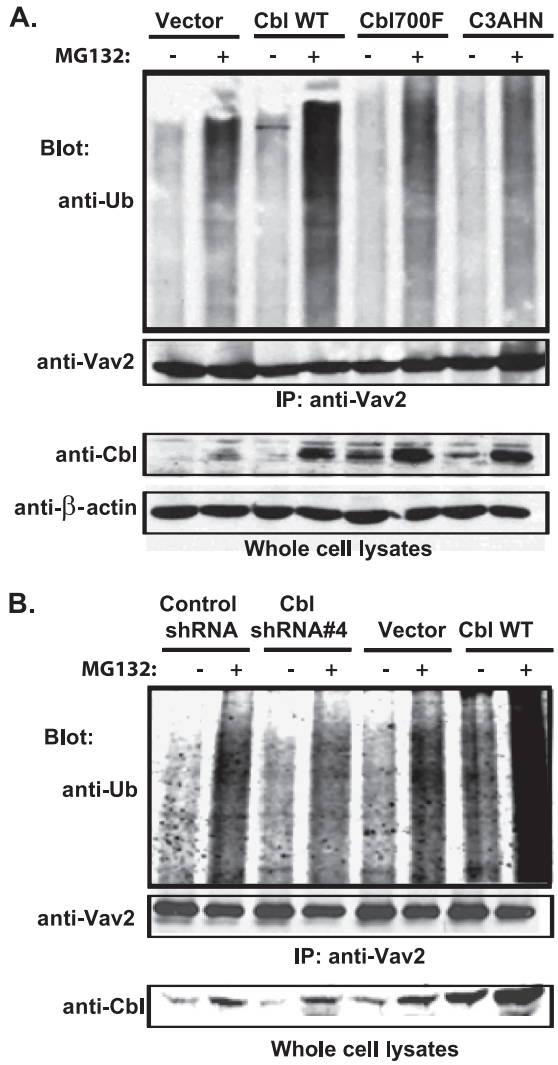

FIGURE 8. **Role of Cbl in Vav2 ubiquitinylation.** 16A5-Tet-On-172F cells with stable expression of vector, wild type Cbl (*A* and *B*), Cbl-Y700F, or Cbl-C3AHN (*A*) or stable expression of control shRNA or Cbl-shRNA#4 (*B*) were treated with DOX for 3 days to induce the expression of Vav2-Y172F. The cells were then treated with DMSO or MG132 (100 μM) for 4 h before lysis. Cell lysates were subjected to IP with anti-Vav2 Abs and immunoblotted for ubiquitin (*Ub*) and Vav2. Whole cell lysates were also blotted for Cbl.

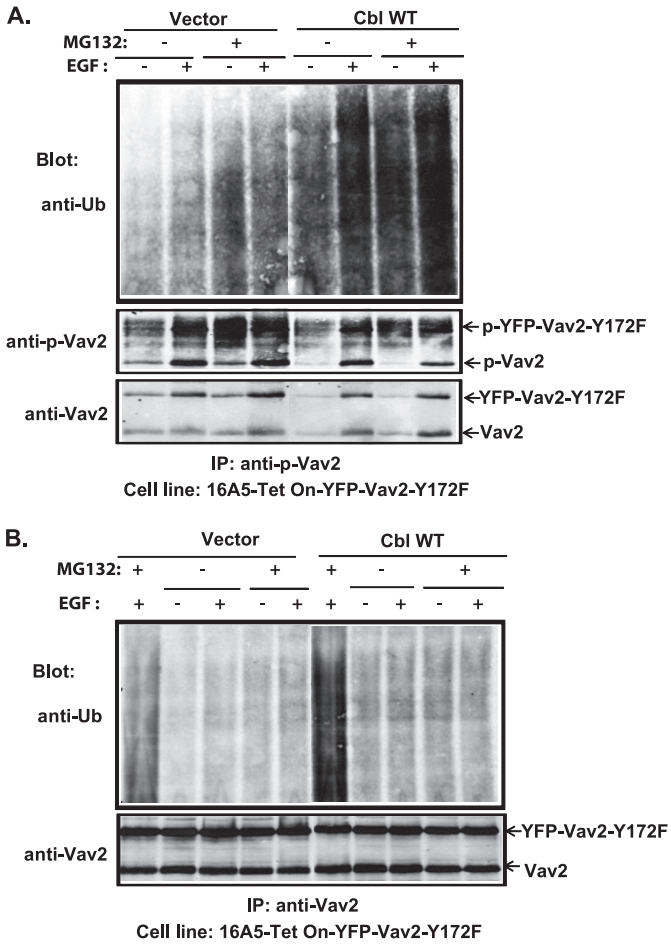

FIGURE 9. **Enhancement of phospho-Vav2 ubiquitinylation by WT Cbl.** 16A5-Tet-On-172F cells stably expressing vector or wild type Cbl were treated with DOX for 2 days to induce expression of Vav2-Y172F and then growth factor-starved for 2 days. The cells were then treated with DMSO or MG132 (20 μM) for 1 h before stimulation with EGF (100 ng/ml) for 10 min. The cells were lysed in RIPA buffer and cell lysates depleted of EGFR by two serial rounds of anti-EGFR IP. The EGFR-depleted lysates were subsequently subjected to IP with anti-phospho-Vav2 antibody. Finally, the post-phospho-Vav2 IP cell lysates (phospho-Vav2-depleted) were subjected to IP with anti-Vav2 antibody (*B 2nd* to *5th* and *7th* to *10th lanes*). The anti-phospho-Vav2 (*A, upper panel*) and the Vav2 IPs (*B, 1st* and *6th lanes* are IPs of whole cell lysates) were immunoblotted for ubiquitin (*Ub*) and reprobed for phospho-Vav2 and Vav2 (*A, middle* and *lower panels* and *B, lower panel*).

EGFR, but some of it is associated with Cbl. These results suggest that, besides the regulation of Vav2 as a complex with EGFR, Cbl can also attenuate Vav2 function through a direct interaction. The direct interaction of Cbl with Vav2 is, however, dependent on EGF stimulation and the Tyr-700 residue in Cbl, suggesting that Cbl-Vav2 interaction is mediated through Vav2 SH2 domain binding to Tyr(P)-700 of Cbl, similar to the previously reported Vav1-Cbl interaction (22, 50). The pool of Vav2 that associates with Cbl independently of EGFR shows no detectable phosphorylation. The biological significance of this association is currently unclear. The canonical activation of Vav proteins is mediated by tyrosine phosphorylation and phospholipid binding (70, 71). Whether the nonphosphorylated and Cbl-associated pool of Vav2 is functionally active has not been directly tested. Our results show that the ubiquitin ligase-deficient Cbl mutants greatly enhanced the Vav2-Y172F-induced morphological transformation of MCF10A (Fig. 7*C*) and 16A5 MECs. This is largely dependent on Tyr-700 of Cbl, implying that direct Cbl-Vav2 interaction regulates the Vav2-mediated cytoskeleton remodeling in a Cbl ubiquitin ligase-dependent manner. Given that natural mutations of Cbl within the linker region or the RING finger domain, both critical for the ubiquitin ligase activity, occur in human leukemia patients (72), it will be of considerable future interest to assess whether such mutants of Cbl can actually increase signaling through Vav proteins. In v-Abl-transformed fibroblasts, phosphorylated Cbl interacts with Vav2 and facilitates fibronectin matrix deposition, which is dependent on Cbl ubiquitin ligase activity (73). Both in the context of parental cells stimulated through EGFR and in the context of Vav2-Y172F-expressing MECs, Cbl proteins attenuate the activation of Rac/Cdc42, cell-cell junctional and actin cytoskeleton remodeling, as well as cell migration. It is therefore reasonable to conclude that Cbl proteins serve as nega-

tive regulators of Vav2 activation through ubiquitinylation and degradation of activated Vav2.

The regulation of actin cytoskeleton by Vav proteins in a variety of biological systems appears critical for their functions in cell signaling (47). For example, Vav1-mediated actin remodeling in T-cells is required for clustering of lipid rafts at the immunological synapse and adequate T-cell receptor signaling (47); Vav2 activation in NIH3T3 cells induces membrane ruffles and stress fibers that control cell migration (44). In epithelial cells (this study), Vav2 is critical for EGF-induced reorganization of junctional actin structures and cell migration; the constitutively active form of Vav2 by itself was able to induce the formation of shorter and thinner peri-junctional actin filaments, which was attenuated by the overexpression of WT Cbl. Such negative regulation of actin reorganization by Cbl may also contribute to its known biological functions in the inhibition of lymphocyte development and activation (74). It is noteworthy that overexpression of a truncated Cbl protein, Cbl-(1–480), in NIH3T3 cells produces a dramatic increase in dorsal ruffle formation accompanied with enhanced Rac activation in response to serum or PDGF stimulation (75). As Cbl-(1–480) lacks C-terminal regions, it is likely that its apparently dominant-negative phenotype relates to the lack of interactions with signaling proteins downstream of RTKs. Although the authors suggested a role of Crk/Crkl adaptor-dependent interactions, it is also possible that these effects relate to a loss of direct negative regulation of Vav-dependent Rac/Cdc42 activation.

Although endocytic down-regulation of EGFR and other RTKs by Cbl family proteins is clearly linked to E3 activity of the latter, both the role of E3 activity in regulating non-kinase targets and the potential consequences of ubiquitin modification remain less clear. By utilizing WT or E3-deficient Cbl proteins, we show that E3 activity of Cbl is required for negative regulation of the Vav2-Rac1/Cdc42 axis. Analyses of an ectopically expressed constitutively active Vav2-Y172F mutant confirmed that Vav2, similar to our earlier studies of Vav1 (22), is a target of Cbl-dependent ubiquitinylation. In lymphocyte systems, PI3K as well as Crk-C3G are now also known to be targeted for ubiquitinylation upon their interaction with Cbl proteins (20, 21). Thus, it is likely that all complexes of Cbl proteins with non-kinase partners are ultimately subjected to ubiquitin modification. The consequences of this ubiquitin modification, however, remain less clear. Our results indicate that phospho-Vav2 is ubiquitinylated in a Cbl E3-dependent manner. Because phospho-Vav2 is responsible for activation of Rac1/Cdc42, disruption of adherens junctions (this study), and disruption of mammary epithelial acini in three-dimensional matrix culture as we have shown previously (49), our finding of Cbl-dependent phospho-Vav2 ubiquitinylation highlights the role of Cbl in the maintenance of epithelial homeostasis during EGFR-mediated cellular remodeling processes.

Notably, contrary to our results and those described by others (discussed above) that collectively support a negative regulatory role of Cbl family proteins on the activation of PI3K, Rap1, and Vav proteins, Cbl appears to play a positive role in the activation of PI3K, Rap1, and Rac1 in v-Abl-transformed NIH3T3 cells with increased cell spreading and migration (76). Although this discrepant function of Cbl is dependent on tyrosine residues that mediate its interaction with PI3K, Crk, and Vav, as well as its E3 ubiquitin ligase activity, it is not clear whether Cbl promotes the ubiquitinylation of PI3K, Crk, or Vav2 in v-Abl-transformed NIH3T3 cells. It remains possible that Cbl may promote the ubiquitinylation of other signaling proteins involved in v-Abl signaling, which facilitate the activation of PI3K, Rap1, and Rac1 in this cell system. Further experiments are needed to understand the discrepant functions of Cbl observed in these different cell systems.

Interestingly, although Cbl family ubiquitin ligases appear to prominently control the biological output of EGFR activation in MECs in terms of Vav2-mediated Rac1/Cdc42 activation, cell-cell junctions, and cell migration, we did not see substantial changes in EGF-dependent cell proliferation. Whether this differential effect reflects compensatory changes in cells or a differential susceptibility of various signaling pathways to Cbl family E3-dependent regulation (perhaps by virtue of direct targeting of associated signaling complexes; Vav2 in the present example) remain open questions for future analyses.

Negative regulation of Vav2 signaling axis by Cbl proteins downstream of a prominent RTK, EGFR, could play significant biological roles in physiology as well as tumorigenesis. In addition to the transforming activity of activated Vav GEFs (47), their knockouts are known to have significant biological phenotypes, especially when multiple family members are perturbed (77). Although a role of Vav2 in breast or other tumors is not known, Vav proteins are known to require binding to phosphatidylinositol (3,4,5)-triphosphate, a product of PI3K that is activated downstream of RTKs (including EGFR) (45). Given a role for EGFR overexpression in breast and other epithelial cancers (3, 5–9, 46), and the identification of activating PI3K mutations associated with several cancers (78), Vav2 may in fact be involved in oncogenic processes. As such, an understanding of the mechanisms of negative regulation of this family of GEFs is likely to be relevant to tumor biology. Notably, Cbl-deficient mice were found to exhibit enhanced branching morphogenesis of the virgin mammary glands (79). Although transplant studies suggest that this phenotype may be related to stromal rather than epithelial cell defects (80), the current results that Cbl proteins control cell migration through the regulation of the Vav2-Rac1/Cdc42 axis raise the possibility that this pathway may be of biological relevance *in vivo*. Our *in vitro* analyses, indicating that Cbl proteins that can interact with Vav2 (but not the ones that lack Tyr-700 or the E3-deficient mutants) could down-regulate the extreme morphological transformation of human MECs, are consistent with this idea. Notably, overexpression of ubiquitin ligase-deficient mutants of Cbl has also been shown to cause epithelial-mesenchymal transition in Madin-Darby canine kidney cells in response to c-MET activation (81), further suggesting that Cbl proteins function in the maintenance of AJs and epithelial homeostasis during the RTK signaling process.

In conclusion, the results presented here reveal that Cbl family proteins play a critical role in the maintenance of epi-

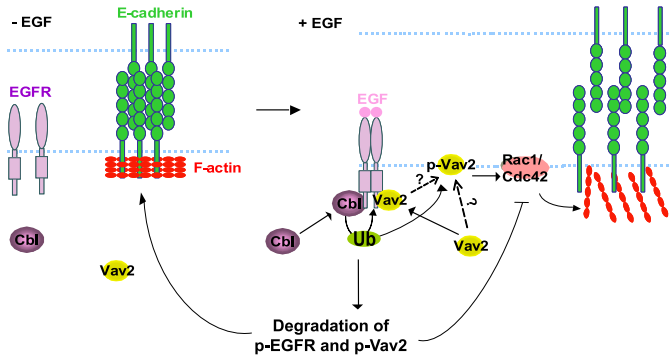

FIGURE 10. **Model of Cbl-dependent stabilization of AJs in EGF-stimulated MECs through negative regulation of EGFR and Vav2 signaling.** MECs form AJs by E-cadherin clustering, which is facilitated by tight circumferential actin cables. EGFR phosphorylates Vav2 that translocates to the cell membrane at the cell-cell junctions and activates Rac1/Cdc42 that reorganizes junctional actin, resulting in de-clustering of E-cadherin and disruption of cell-cell adhesions. Attenuation of Rac1/Cdc42 activation is partially achieved by Cbl-mediated ubiquitinylation of EGFR resulting in attenuation of phosphorylated Vav2. Cbl can additionally lead to ubiquitinylation (*Ub*) and degradation of p-Vav2 resulting in its removal from the junctional membrane, therefore temporally and spatially restricting Rac1/Cdc42 activation and reorganization of junctional actin cytoskeleton. This attenuation is hypothesized to serve as a physiological barrier to prevent excessive reorganization of junctional actin cytoskeleton and complete loss of AJs during EGF-induced MEC remodeling process.

thelial AJs through attenuation of the EGFR-Vav2-Rac1/Cdc42 signaling axis, suggesting an important role of Cbl proteins in controlling cell-cell junctions, actin cytoskeleton remodeling, and migration responses downstream of EGFR (Fig. 10). Future studies of the model systems described here could help in elucidating the biological roles of Cbl-mediated, and ubiquitinylation-dependent, negative regulation of components of EGFR signaling and other RTKs in a biologically meaningful context.

Acknowledgments—We thank Drs. Senthil Muthuswamy (MCF10A cells), Jonathan Higgins and Michael Brenner (anti-E-cadherin hybridoma), Martin Schwartz (GST-RBD), John G. Collard (GST-PBD), and Brian Druker (4G10 antibody) for gifts of critical reagents. We thank Dr. Aharon Solomon for help with statistical analyses and other members of the Band laboratories for helpful suggestions and discussion. We thank Janice Taylor and James Talaska for providing assistance with confocal microscopy. The confocal laser scanning microscope and other core facilities used in this study were supported by Nebraska Research Initiative and University of Nebraska Medical Center-Eppley Cancer Center Core Support Grant from the NCI, National Institutes of Health.

REFERENCES

1. Wells, A. (1999) *Int. J. Biochem. Cell Biol.* **31,** 637–643
2. Yarden, Y., and Sliwkowski, M. X. (2001) *Nat. Rev. Mol. Cell Biol.* **2,** 127–137
3. Arteaga, C. (2003) *Semin. Oncol.* **30,** Suppl. 7, 3–14
4. Jost, M., Kari, C., and Rodeck, U. (2000) *Eur. J. Dermatol.* **10,** 505–510
5. Yarden, Y. (2001) *Eur. J. Cancer* **37,**S3–S8
6. Chrysogelos, S. A., and Dickson, R. B. (1994) *Breast Cancer Res. Treat.* **29,** 29–40
7. Khazaie, K., Schirrmacher, V., and Lichtner, R. B. (1993) *Cancer Metastasis Rev.* **12,** 255–274
8. Magkou, C., Nakopoulou, L., Zoubouli, C., Karali, K., Theohari, I., Bakarakos, P., and Giannopoulou, I. (2008) *Breast Cancer Res.* **10,** R49
9. Rajkumar, T., and Gullick, W. J. (1994) *Breast Cancer Res. Treat.* **29,** 3–9
10. Sorkin, A., and Goh, L. K. (2008) *Exp. Cell Res.* **314,** 3093–3106
11. Schmidt, M. H., and Dikic, I. (2005) *Nat. Rev. Mol. Cell Biol.* **6,** 907–918
12. Rubin, C., Gur, G., and Yarden, Y. (2005) *Cell Res.* **15,** 66–71
13. Duan, L., Miura, Y., Dimri, M., Majumder, B., Dodge, I. L., Reddi, A. L., Ghosh, A., Fernandes, N., Zhou, P., Mullane-Robinson, K., Rao, N., Donoghue, S., Rogers, R. A., Bowtell, D., Naramura, M., Gu, H., Band, V., and Band, H. (2003) *J. Biol. Chem.* **278,** 28950–28960
14. Ettenberg, S. A., Magnifico, A., Cuello, M., Nau, M. M., Rubinstein, Y. R., Yarden, Y., Weissman, A. M., and Lipkowitz, S. (2001) *J. Biol. Chem.* **276,** 27677–27684
15. Waterman, H., Levkowitz, G., Alroy, I., and Yarden, Y. (1999) *J. Biol. Chem.* **274,** 22151–22154
16. Waterman, H., Katz, M., Rubin, C., Shtiegman, K., Lavi, S., Elson, A., Jovin, T., and Yarden, Y. (2002) *EMBO J.* **21,** 303–313
17. Eden, E. R., White, I. J., and Futter, C. E. (2009) *Biochem. Soc. Trans.* **37,** 173–177
18. Rodahl, L. M., Stuffers, S., Lobert, V. H., and Stenmark, H. (2009) *Biochem. Soc. Trans.* **37,** 137–142
19. Saksena, S., Sun, J., Chu, T., and Emr, S. D. (2007) *Trends Biochem. Sci.* **32,** 561–573
20. Fang, D., and Liu, Y. C. (2001) *Nat. Immunol.* **2,** 870–875
21. Shao, Y., Elly, C., and Liu, Y. C. (2003) *EMBO Rep.* **4,** 425–431
22. Miura-Shimura, Y., Duan, L., Rao, N. L., Reddi, A. L., Shimura, H., Rottapel, R., Druker, B. J., Tsygankov, A., Band, V., and Band, H. (2003) *J. Biol. Chem.* **278,** 38495–38504
23. Singh, A. J., Meyer, R. D., Navruzbekov, G., Shelke, R., Duan, L., Band, H., Leeman, S. E., and Rahimi, N. (2007) *Proc. Natl. Acad. Sci. U.S.A.* **104,** 5413–5418
24. Reddi, A. L., Ying, G., Duan, L., Chen, G., Dimri, M., Douillard, P., Druker, B. J., Naramura, M., Band, V., and Band, H. (2007) *J. Biol. Chem.* **282,** 29336–29347
25. Stampfer, M. R., Pan, C. H., Hosoda, J., Bartholomew, J., Mendelsohn, J., and Yaswen, P. (1993) *Exp. Cell Res.* **208,** 175–188
26. Bissell, M. J., Radisky, D. C., Rizki, A., Weaver, V. M., and Petersen, O. W. (2002) *Differentiation* **70,** 537–546
27. Debnath, J., and Brugge, J. S. (2005) *Nat. Rev. Cancer* **5,** 675–688
28. Nelson, W. J. (2003) *Nature* **422,** 766–774
29. McNeill, H., Ozawa, M., Kemler, R., and Nelson, W. J. (1990) *Cell* **62,** 309–316
30. De Vries, W. N., Evsikov, A. V., Haac, B. E., Fancher, K. S., Holbrook, A. E., Kemler, R., Solter, D., and Knowles, B. B. (2004) *Development* **131,** 4435–4445
31. Gumbiner, B. M. (2005) *Nat. Rev. Mol. Cell Biol.* **6,** 622–634
32. Birchmeier, W., Hulsken, J., and Behrens, J. (1995) *CIBA Found. Symp.* **189,** 124–136; discussion 136–41, 174–176
33. Wodarz, A., and Näthke, I. (2007) *Nat. Cell Biol.* **9,** 1016–1024
34. Hirohashi, S., and Kanai, Y. (2003) *Cancer Sci.* **94,** 575–581
35. Hazan, R. B., and Norton, L. (1998) *J. Biol. Chem.* **273,** 9078–9084
36. Lu, Z., Ghosh, S., Wang, Z., and Hunter, T. (2003) *Cancer Cell* **4,** 499–515
37. Schmidt, A., and Hall, A. (2002) *Genes Dev.* **16,** 1587–1609
38. Rossman, K. L., Der, C. J., and Sondek, J. (2005) *Nat. Rev. Mol. Cell Biol.* **6,** 167–180
39. Schmitz, A. A., Govek, E. E., Böttner, B., and Van Aelst, L. (2000) *Exp. Cell Res.* **261,** 1–12
40. Takaishi, K., Sasaki, T., Kato, M., Yamochi, W., Kuroda, S., Nakamura, T., Takeichi, M., and Takai, Y. (1994) *Oncogene* **9,** 273–279
41. Kamei, T., Matozaki, T., Sakisaka, T., Kodama, A., Yokoyama, S., Peng, Y. F., Nakano, K., Takaishi, K., and Takai, Y. (1999) *Oncogene* **18,** 6776–6784
42. Braga, V. M., Betson, M., Li, X., and Lamarche-Vane, N. (2000) *Mol. Biol. Cell* **11,** 3703–3721
43. Schiller, M. R. (2006) *Cell. Signal.* **18,** 1834–1843
44. Liu, B. P., and Burridge, K. (2000) *Mol. Cell. Biol.* **20,** 7160–7169
45. Tamás, P., Solti, Z., Bauer, P., Illés, A., Sipeki, S., Bauer, A., Faragó, A., Downward, J., and Buday, L. (2003) *J. Biol. Chem.* **278,** 5163–5171
46. Abe, K., Rossman, K. L., Liu, B., Ritola, K. D., Chiang, D., Campbell, S. L.,

Burridge, K., and Der, C. J. (2000) *J. Biol. Chem.* **275,** 10141–10149
47. Hornstein, I., Alcover, A., and Katzav, S. (2004) *Cell. Signal.* **16,** 1–11
48. Pandey, A., Podtelejnikov, A. V., Blagoev, B., Bustelo, X. R., Mann, M., and Lodish, H. F. (2000) *Proc. Natl. Acad. Sci. U.S.A.* **97,** 179–184
49. Duan, L., Chen, G., Virmani, S., Ying, G., Raja, S. M., Chung, B. M., Rainey, M. A., Dimri, M., Ortega-Cava, C. F., Zhao, X., Clubb, R. J., Tu, C., Reddi, A. L., Naramura, M., Band, V., and Band, H. (2010) *J. Biol. Chem.* **285,** 1555–1568
50. Marengère, L. E., Mirtsos, C., Kozieradzki, I., Veillette, A., Mak, T. W., and Penninger, J. M. (1997) *J. Immunol.* **159,** 70–76
51. Band, V., and Sager, R. (1989) *Proc. Natl. Acad. Sci. U.S.A.* **86,** 1249–1253
52. Soule, H. D., Maloney, T. M., Wolman, S. R., Peterson, W. D., Jr., Brenz, R., McGrath, C. M., Russo, J., Pauley, R. J., Jones, R. F., and Brooks, S. C. (1990) *Cancer Res.* **50,** 6075–6086
53. Fernandez-Zapico, M. E., Gonzalez-Paz, N. C., Weiss, E., Savoy, D. N., Molina, J. R., Fonseca, R., Smyrk, T. C., Chari, S. T., Urrutia, R., and Billadeau, D. D. (2005) *Cancer Cell* **7,** 39–49
54. Fukazawa, T., Miyake, S., Band, V., and Band, H. (1996) *J. Biol. Chem.* **271,** 14554–14559
55. Bao, J., Gur, G., and Yarden, Y. (2003) *Proc. Natl. Acad. Sci. U.S.A.* **100,** 2438–2443
56. Zhang, J., Bárdos, T., Li, D., Gál, I., Vermes, C., Xu, J., Mikecz, K., Finnegan, A., Lipkowitz, S., and Glant, T. T. (2002) *J. Immunol.* **169,** 2236–2240
57. Pennock, S., and Wang, Z. (2008) *Mol. Cell. Biol.* **28,** 3020–3037
58. Jeanes, A., Gottardi, C. J., and Yap, A. S. (2008) *Oncogene* **27,** 6920–6929
59. Thiery, J. P., and Chopin, D. (1999) *Cancer Metastasis Rev.* **18,** 31–42
60. Thiery, J. P. (2002) *Nat. Rev. Cancer* **2,** 442–454
61. Takeichi, M. (1993) *Curr. Opin. Cell Biol.* **5,** 806–811
62. Behrens, J. (1993) *Breast Cancer Res. Treat.* **24,** 175–184
63. Fukata, M., and Kaibuchi, K. (2001) *Nat. Rev. Mol. Cell Biol.* **2,** 887–897
64. Arthur, W. T., Noren, N. K., and Burridge, K. (2002) *Biol. Res.* **35,** 239–246
65. Braga, V. M., Machesky, L. M., Hall, A., and Hotchin, N. A. (1997) *J. Cell Biol.* **137,** 1421–1431
66. Brunton, V. G., MacPherson, I. R., and Frame, M. C. (2004) *Biochim. Biophys. Acta* **1692,** 121–144
67. Evers, E. E., Zondag, G. C., Malliri, A., Price, L. S., ten Klooster, J. P., van der Kammen, R. A., and Collard, J. G. (2000) *Eur. J. Cancer* **36,** 1269–1274
68. Fujita, Y., and Braga, V. (2005) *Novartis Found. Symp.* **269,** 144–155; discussion 155–8, 223–230
69. Jou, T. S., Schneeberger, E. E., and Nelson, W. J. (1998) *J. Cell Biol.* **142,** 101–115
70. Han, J., Luby-Phelps, K., Das, B., Shu, X., Xia, Y., Mosteller, R. D., Krishna, U. M., Falck, J. R., White, M. A., and Broek, D. (1998) *Science* **279,** 558–560
71. Bustelo, X. R. (1996) *Crit. Rev. Oncog.* **7,** 65–88
72. Bacher, U., Haferlach, C., Schnittger, S., Kohlmann, A., Kern, W., and Haferlach, T. (2010) *Ann. Hematol.* **89,** 643–652
73. Teckchandani, A. M., Feshchenko, E. A., and Tsygankov, A. Y. (2001) *Oncogene* **20,** 1739–1755
74. Huang, F., and Gu, H. (2008) *Immunol. Rev.* **224,** 229–238
75. Scaife, R. M., Courtneidge, S. A., and Langdon, W. Y. (2003) *J. Cell Sci.* **116,** 463–473
76. Lee, H., Gaughan, J. P., and Tsygankov, A. Y. (2008) *Int. J. Biochem. Cell Biol.* **40,** 1930–1943
77. Turner, M. (2002) *Adv. Exp. Med. Biol.* **512,** 29–34
78. Zhao, L., and Vogt, P. K. (2008) *Oncogene* **27,** 5486–5496
79. Murphy, M. A., Schnall, R. G., Venter, D. J., Barnett, L., Bertoncello, I., Thien, C. B., Langdon, W. Y., and Bowtell, D. D. (1998) *Mol. Cell. Biol.* **18,** 4872–4882
80. Crowley, M. R., Bowtell, D., and Serra, R. (2005) *Dev. Biol.* **279,** 58–72
81. Fournier, T. M., Lamorte, L., Maroun, C. R., Lupher, M., Band, H., Langdon, W., and Park, M. (2000) *Mol. Biol. Cell* **11,** 3397–3410